Optics Communications 283 (2010) 2385–2389

Contents lists available at ScienceDirect

Optics Communications

journal homepage: www.elsevier.com/locate/optcom

Periodic surface nanostructures on polycrystalline ZnO induced by femtosecond laser pulses

Weiwei Liang [a,b], Feng Chen [a,b,*], Hao Bian [a,b], Qing Yang [c], Hewei Liu [a,b], Xianhua Wang [a,b], Jinhai Si [a,b], Xun Hou [a,b]

[a] Key Laboratory for Physical Electronics and Devices of the Ministry of Education, Shaanxi Province, School of Electronics and Information Engineering, Xi'an Jiaotong University, No. 28, Xianning West Road, Xi'an 710049, PR China

[b] Key Laboratory of Photonics Technology for Information, Shaanxi Province, School of Electronics and Information Engineering, Xi'an Jiaotong University, No. 28, Xianning West Road, Xi'an 710049, PR China

[c] State Key Laboratory for Manufacturing Systems Engineering, School of Mechanical Engineering, Xi'an Jiaotong University, No. 28, Xianning West Road, Xi'an 710049, PR China

ARTICLE INFO

Article history:
Received 26 October 2009
Received in revised form 29 January 2010
Accepted 1 February 2010

Keywords:
Femtosecond laser pulses
Periodic surface nanostructures
Polycrystalline ZnO
Nanofabrication
Surface modification

ABSTRACT

Periodic surface nanostructures induced by femtosecond laser pulses on polycrystalline ZnO are presented. By translating the sample line-by-line under appropriate irradiation conditions, grating-like nanostructures with an average period of 160 nm are fabricated. The dependence of surface morphologies on the processing parameters, such as laser fluence, pulse number and laser polarization, are studied by scanning electronic microscope (SEM). In addition, photoluminescence (PL) analysis at room-temperature indicates that the PL intensity of the irradiated area increases significantly compared with the un-irradiated area. Using femtosecond laser pulses irradiation to fabricate periodic surface nanostructures on polycrystalline ZnO is efficient, simple and low cost, which shows great potential applications in ZnO-based optoelectronic devices.

1. Introduction

Nanofabrication techniques have been attracting abundant research interests for the novel electronic, optical and mechanical properties of various nanostructures exhibiting broad potential applications in numerous fields, such as catalysis, clean energy and life sciences [1–3]. In a mass of physical, chemical and mechanical techniques for nanofabrication, the laser-assisted methods have shown to be efficient and environmentally friendly, which aroused many researchers' greatest attention [4–6]. For example, laser-induced periodic surface structures (LIPSS) have been studied on various materials, and different nanostructures can be fabricated by laser irradiation with different processing parameters [7–9]. A wide range of laser sources, especially the ultra-short laser pulses owe to its minimal thermal and mechanical damages, have been used to fabricate spatially periodic structures on the surface of metals, semiconductors, dielectrics and polymers [10–13].

Zinc oxide (ZnO), with a band gap of 3.37 eV and a large exciton binding energy of 60 MeV at room-temperature, has attracted a great deal of interests in the past decades due to its wide applications in field emission devices, UV light emitting diodes, nanogenerators and solar cells [14,15]. Many works concentrated on formation of nanostructures on ZnO because it exhibited the most splendid and abundant configurations of nanostructures that one material can form [16]. Recently, femtosecond laser became a new tool to produce nanostructures on various bulk solids, which would also provide us a controllable method to fabricate ZnO nanostructures. When the laser fluence slightly exceeded the ablation threshold, uniform nanostructures were formed on irradiated regions efficiently. Other than some reports on femtosecond laser-induced LIPSS in ZnO thin films [17,18], a series of publications have focused on the formation of LIPSS on the surface of single-crystalline ZnO upon irradiation with focused Ti:sapphire femtosecond laser pulses [19–22]. Reviewing previous works, most of them were concentrated on the single-crystalline ZnO bulks with smooth surface, while seldom reported the formation of nanostructures on polycrystalline ZnO bulks with rough surfaces, which are lower cost and easier to be prepared.

In this paper, we fabricated periodic surface nanostructures on polycrystalline ZnO with original surface roughness by scanning the femtosecond laser pulses in a simple line-scan mode. Scanning electronic microscope (SEM) investigations demonstrated that uniform nanostructures with an average period of 160 nm have been successfully induced on rough surface of polycrystalline ZnO bulks. Furthermore, we studied the dependence of surface morphologies

* Corresponding author. Tel./fax: +86 29 82665105.
E-mail address: chenfeng@mail.xjtu.edu.cn (F. Chen).

0030-4018/$ - see front matter © 2010 Elsevier B.V. All rights reserved.
doi:10.1016/j.optcom.2010.02.003

on the processing parameters, such as laser fluence, pulse number and polarization. Finally, the room-temperature photoluminescence (PL) measurements were used to exploring the emission characteristics of the areas before and after the femtosecond laser irradiation, the results indicated that the presence of nanostructures could significantly enhance the PL intensity.

2. Materials and experimental procedures

A polycrystalline ZnO plate with diameter of 15 mm and thickness of 2 mm was used in our experiments. The plate was sintered by ZnO powder with the purity of 99.999%, and then prepared under 1×10^3 MPa pressure in clean environment.

The experimental setup was shown in Fig. 1. A model-locked Ti:sapphire multi-pass amplifying system (FEMTOPOWER compact Pro, FEMTOLASERS) was used to generate femtosecond laser pulses at 1 kHz repetition rate with the central wavelength of 800 nm. A 20× microscope objective (Nikon, N.A. = 0.45) was used to focus the laser beam at normal incidence onto the sample which was mounted on a computer controlled 3D translation stage with a resolution of 0.04 μm. The energy of the incident laser could be continuously varied by a variable attenuator, and the polarization of the laser could be changed by a half-wave plate. The laser fluence was monitored by a powermeter. The number of laser shots was controlled by an electromechanical shutter. The pulse can be changed by adjusting the prism compressor inside the amplifier unit, to introduce appropriate dispersion pre-compensation depends on the final pulse duration reached to the sample surface. And the laser pulse duration was measured by an autocorrelator (Femtometer, FEMTOLASERS), so we achieved a pulse duration of 30 fs (FWHM) pulses focused by the 20× (Nikon, N.A. = 0.45) microscope objective.

After the laser irradiation, the sample was rinsed in deionized water for 5 min to clean the residual debris. The morphologies of the nano-structured areas were characterized by a SEM (JEOL, JSM-7000F), and the PL spectrum was performed by using an He–Cd laser (λ = 325 nm) as the excitation source at room-temperature.

3. Results and discussion

The dependence of surface morphologies on incident laser fluence was shown in Fig. 2. Fig. 2(a) shows the morphology of sample surface before laser irradiation, the sample surface exhibits regular roughness with grain size distributes in the range of 2–3 μm. After laser irradiation, the grating-like nanostructures were observed on the irradiated areas with the laser fluence of (b) 2.0 J/cm^2, (c) 2.6 J/cm^2 and (d) 3.1 J/cm^2, respectively. In Fig. 2(b), the grating-like nanostructures were formed on the top of the grains at lower laser fluence, and the cavities still could be seen under the nano-structured surface layer. With the laser fluence increasing, the nano-grating arrays were observed on the sample surface, and the surface retained the original roughness, as shown in Fig. 2(c). If the laser fluence further increased, as shown in Fig. 2(d), tailored nano-grating arrays with controlled shape and ordered morphology could be fabricated.

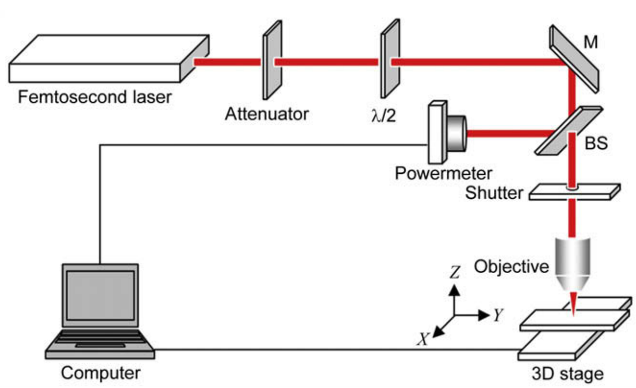

Fig. 1. Experimental setup. It consists of a femtosecond laser resource, a variable attenuator, a half-wave plate, a mechanical shutter and a microscope objective. The sample was positioned on a mechanical 3D stage controlled by a computer. The laser fluence was monitored by a powermeter.

Fig. 3 shows the dependence of surface morphologies on pulse number. Fig. 3(a) shows the ZnO surface after irradiation by 3×10^5 linear polarized femtosecond laser pulses with the laser fluence of 3.1 J/cm^2. The grating-like nanostructures with a period of about 160 nm can be observed in the irradiated area. This period is measured as about 20% of the laser wavelength (800 nm). When the number of the incident laser pulses increased to 6×10^5, the grating-like nanostructures still appeared in the irradiated area, as shown in Fig. 3(c), but the morphology of the nano-gratings became rougher. A mass of nanometer-sized protuberances can be found on the surface of irradiated region, which might be attributed to the redeposition of ablation debris. Fig. 3(b) and (d) were the higher magnification images of Fig. 3(a) and (c), respectively.

There are many reports concentrated on the formation mechanisms of femtosecond laser-induced periodic surface structures on smooth surface [23–26]. It was generally proposed that periodic structures are determined by the interference of the incident laser beam with the surface scattered wave. However, in our experiment, the uniform ZnO nano-gratings are fabricated on the loose and grain-covered surface. The interference model can only explain the ripples formed on the top of the grains at lower laser fluence. With the increasing of laser fluence, nano-gratings will be gradually formed in the cavities where the incident laser could not reach. Reif et al. suggested that the ripples were due to self-organization structure formation during the relaxation of the highly non-equilibrium surface after explosive positive particles emission [27]. The particles might fill the cavities and smooth the surface, so the nano-grating arrays can be formed on the loose and grain-covered ZnO surface. So, we propose such nano-gratings formed on porous surface are a combined result of interference and self-organization. At lower laser fluence, as shown in Fig. 2(b), nano-gratings are formed only on the top of the grains. The incident laser only excites the electrons of the system at first, and the ions emit after electronic excitation converted into ion kinetic energy. The nano-gratings should attribute to the interference of the incident laser with the scattered light caused by the roughness of the surface, and the density of ions induced by the laser is very low. With the laser fluence increasing, as shown in Fig. 2(c), nano-gratings gradually are formed all over the irradiated area, and the redeposition of ablation debris indicates that the ion density is high enough, so we believe the self-organization plays an important role in the formation process. The self-organization is consisting of a competition between surface roughing due to ablation and smoothing because of atomic diffusion [24]. When the incident laser reached to a higher fluence, as shown in Fig. 2(d), the atomic surface diffusion process may play a dominant role and tend to smooth the surface by filling the cavities with diffused particles. The grating-like nanostructures are formed due to self-organization structure formation during the relaxation of the highly non-equilibrium surface after explosive intense femtosecond laser pulses irradiation. It can be seen from Fig. 3, the nano-gratings cover the whole irradiated area under self-organization process. Detailed mechanism is still necessary and under way to understand the phenomenon.

We also produced multi-shot craters on the ZnO by changing the laser polarization. The laser fluence was 3.1 J/cm^2 and the number of incident laser pulses was 3×10^5. The grating-like nano-

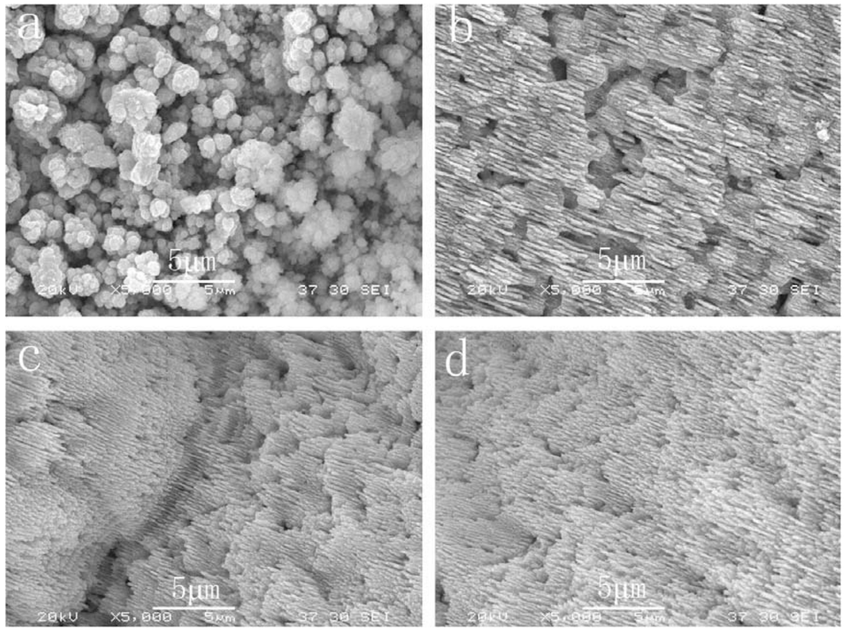

Fig. 2. The dependence of surface morphologies on incident laser fluence. (a) The morphology of the un-irradiated area. The influence of laser fluence on the morphologies of the nano-gratings formed by the irradiation of linearly polarized laser with the fluences of (b) 2.0 J/cm^2, (c) 2.6 J/cm^2 and (d) 3.1 J /cm^2. The number of incident laser pulses was 3×10^5.

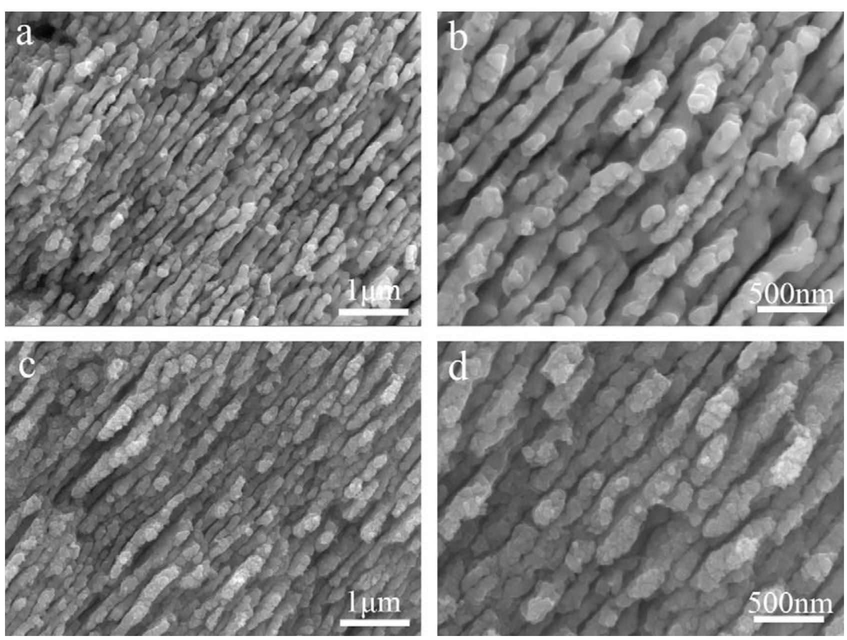

Fig. 3. The SEM images of the grating-like nanostructures induced by femtosecond laser under different number of laser pulses: (a) 3×10^5 and (c) 6×10^5 linear polarization laser pulses. The laser fluence was 3.1 J/cm^2. (b) and (d) were the higher magnification images of (a) and (c), respectively.

structures were fabricated in the craters, as shown in Fig. 4. The orientation of the periodic nanostructures was perpendicular to the direction of laser polarization, and the polarization directions were shown by the arrows.

Subsequently, we fabricated a large-area uniform nanostructure on the sample surface using the simple line-scan method. In our experiments, the laser beam scanned along the orientation perpendicular to the laser polarization and the interspacing of the scanning lines was set to 2 μm. In order to obtain a fine surface morphology, the laser fluence and scanning speed were set to 3.1 J/cm^2 and 20 μm/s, respectively. Fig. 5 shows the SEM images of ZnO nanostructures and the inset shows the top view of the irradiated area. We can see that the uniform nanostructures were prepared on the ZnO plate in a square region with dimensions of 200 μm × 200 μm. The surface morphology of the treated area is smooth; grains and cavities rarely can be found. The experimental results indicated that femtosecond laser is an efficient tool to fabricate large-area uniform nanostructures. It should be noted that by altering some parameters, the nanostructures could be controlled conveniently.

The room-temperature PL measurements are employed to investigate emission characteristics of ZnO using an He–Cd

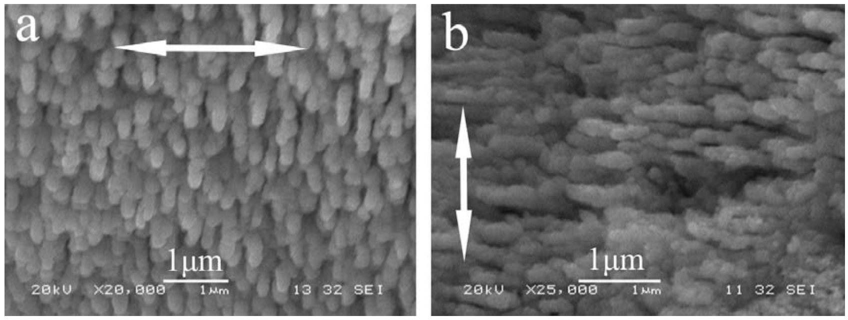

Fig. 4. The SEM images of ZnO surface after irradiated with different laser polarization directions. The laser polarization directions are shown by the arrows. The laser fluence was 3.1 J/cm^2 and the number of incident laser pulses was 3×10^5.

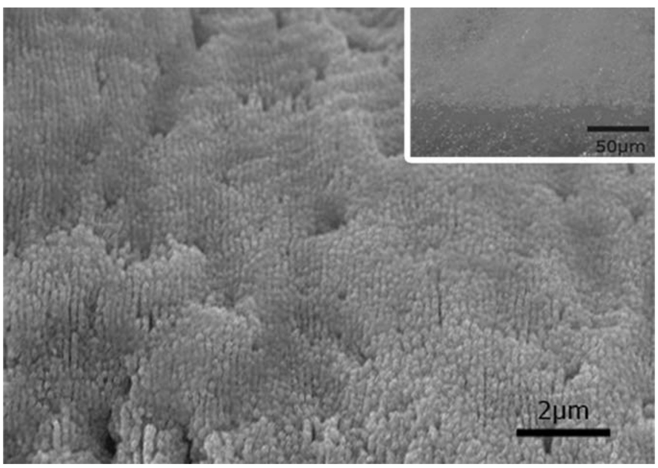

Fig. 5. The SEM images of a ZnO nanostructures area achieved in line-scan mode. The inset shows the top view of the irradiated area. The laser fluence was 3.1 J/cm^2, the scanning speed was 20 μm/s and interval of two adjacent scanning lines was 2 μm.

laser (325 nm) as the excitation source. Fig. 6 shows the room-temperature PL spectra of ZnO. It can be seen from Fig. 6 that the PL intensity of the irradiated area increase significantly compared with the un-irradiated area. Strong emission at 387 nm is observed for both of them. In addition, we observe that the green emission intensity at 520 nm increase notably higher than the UV emission on irradiated area. It is well known that the UV emission peak usually originates form the near band-edge emission from the recombination of free excitons, the green emission broadband centered at about 520 nm is attributed to the singly ionized oxygen vacancy in ZnO and the emission results from the radiative recombination of a photon-generated hole with an electron occupying the oxygen vacancy [14]. The progressive increase of the green emission relative to the UV emission on irradiated area suggests that there is a greater fraction of oxygen vacancies on nano-structured region. In our experiment, intense femtosecond laser pulses are employed to induce periodic nanostructures on the ZnO surface. Comparing with the bulk ZnO, nano-structured ZnO have a higher surface to volume ratio. We believe a higher surface to volume ratio for nano-structured region might favor a higher level of surface and sub-surface oxygen vacancy [28]. The higher surface to volume ratio, the stronger the green emission, whereas the peak remains centered at 520 nm. In addition, it has been reported that the luminescence quantum efficiency of nanostructures increased with decreasing structure size [29]. So, the enhancement observed in the PL intensity on nano-structured region is attributed to the higher surface to volume ratio, as well as the higher luminescence quantum efficiency.

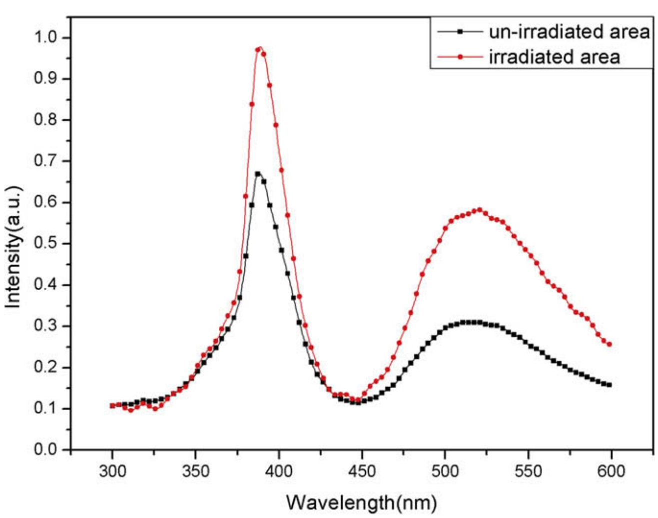

Fig. 6. Measured room-temperature photoluminescence spectrum of irradiated area and un-irradiated area. The PL spectrum was achieved using an He–Cd laser (325 nm) as the excitation source under same excitation density and excitation angle.

4. Conclusions

In summary, we presented the investigations of periodic nanostructures on polycrystalline ZnO surface fabricated by femtosecond laser pulses irradiation. The laser fluence, pulse number and polarization were changed to study the influence on the morphology of the ZnO nanostructures. We suggest that the structure formation might be a combined result of interference and self-organization. The room-temperature PL spectrums exhibited that the PL intensity of the irradiated area was increased significantly. These findings may provide useful information for understanding of the formation mechanisms of femtosecond laser-induced periodic nanostructures and strengthen the interest of ZnO-based optoelectronic device applications.

Acknowledgments

The authors gratefully acknowledge the financial support for this work provided by National High Technology R&D Program of China under the Grant No. 2009AA04Z305, and the National Science Foundation of China under the Grant Nos. 60678011, 10674107 and 60876038.

References

[1] P. Gao, Y. Ding, Z. Wang, Nano Lett. 3 (2003) 1315.
[2] V. Jayawarna, M. Ali, T. Jowitt, A. Miller, A. Saiani, J. Gough, R. Ulijn, Adv. Mater. 18 (2006) 611.
[3] P. Kamat, J. Phys. Chem. C 111 (2007) 2834.
[4] Q. Xia, C. Keimel, H. Ge, Z. Yu, W. Wu, S. Chou, Appl. Phys. Lett. 83 (2003) 4417.
[5] K. Yi, Z. Yang, Y. Lu, J. Appl. Phys. 103 (2008) 054307.
[6] Y. Zhang, R. Russo, S. Mao, Appl. Phys. Lett. 87 (2005) 133115.
[7] M. Birnbaum, J. Appl. Phys. 36 (1965) 3688.
[8] J.E. Sipe, J.F. Young, J.S. Preston, H.M.V. Driel, Phys. Rev. B 27 (1983) 1141.
[9] M. Shen, C. Crouch, J. Carey, E. Mazur, Appl. Phys. Lett. 85 (2004) 5694.
[10] H. Iwase, S. Kokubo, S. Juodkazis, H. Misawa, Opt. Express 17 (2009) 4388.
[11] T. Jia, H. Chen, M. Huang, F. Zhao, J. Qiu, R. Li, Z. Xu, X. He, J. Zhang, H. Kuroda, Phys. Rev. B 72 (2005) 125429.
[12] G. Miyaji, K. Miyazaki, Opt. Express 16 (2008) 16265.
[13] M. Ivanov, P. Rochon, Appl. Phys. Lett. 84 (2004) 4511.
[14] A.B. Djurisic, Y.H. Leung, Small 2 (2006) 944.
[15] Ü. Özgur, Y.I. Alivov, C. Liu, A. Teke, M.A. Reshchikov, S. Dogan, V. Avrutin, S.J. Cho, H. Morkoc, J. Appl. Phys. 98 (2005) 041301.
[16] Z.L. Wang, Mater. Sci. Eng. R-Rep. 64 (2009) 33.
[17] R. Grunwald, U. Neumann, W. Seeber, H. Lange, J. Mosnier, R. O'Haire, E. McGlynn, Phys. Chem. Glasses 48 (2007) 134.
[18] M. Zamfirescu, M. Ulmeanu, F. Jipa, O. Cretu, A. Moldovan, G. Epurescu, M. Dinescu, R. Dabu, J. Laser Micro/Nanoeng. 4 (2009) 7.
[19] X.D. Guo, R.X. Li, Y. Hang, Z.Z. Xu, B.K. Yu, H.L. Ma, X.W. Sun, Mater. Lett. 61 (2007) 4583.
[20] X.D. Guo, R.X. Li, Y. Hang, Z.Z. Xu, B.K. Yu, H.L. Ma, B. Lu, X.W. Sun, Mater. Lett. 62 (2008) 1769.
[21] M. Huang, F.L. Zhao, Y. Cheng, N.S. Xu, Z.Z. Xu, Opt. Express 16 (2008) 19354.
[22] D. Dufft, A. Rosenfeld, S.K. Das, R. Grunwald, J. Bonse, J. Appl. Phys. 105 (2009) 034908.
[23] M. Csete, O. Marti, Z. Bor, Appl. Phys. A 73 (2001) 521.
[24] J. Reif, O. Varlamova, F. Costache, Appl. Phys. A 92 (2008) 1019.
[25] Y. Dong, P. Molian, Appl. Phys. Lett. 84 (2004) 10.
[26] X. Wu, T. Jia, F. Zhao, M. Huang, N. Xu, H. Kuroda, Z. Xu, Appl. Phys. A 86 (2007) 491.
[27] J. Reif, F. Costache, M. Henyk, S. Pandelov, Appl. Surf. Sci. 197 (2002) 891.
[28] P. Yang, H. Yan, S. Mao, R. Russo, J. Johnson, R. Saykally, N. Morris, J. Pham, R. He, H. Choi, Adv. Funct. Mater. 12 (2002) 323.
[29] A. Van Dijken, J. Makkinje, A. Meijerink, J. Lumin. 92 (2001) 323.